THE REUVEN RAMATY HIGH-ENERGY SOLAR SPECTROSCOPIC IMAGER (RHESSI)

R. P. LIN[1,2], B. R. DENNIS[3], G. J. HURFORD[1], D. M. SMITH[1], A. ZEHNDER[4],
P. R. HARVEY[1], D. W. CURTIS[1], D. PANKOW[1], P. TURIN[1], M. BESTER[1],
A. CSILLAGHY[1,9], M. LEWIS[1], N. MADDEN[5], H. F. VAN BEEK[6], M. APPLEBY[7],
T. RAUDORF[8], J. McTIERNAN[1], R. RAMATY[3,10], E. SCHMAHL[3,15],
R. SCHWARTZ[3,16], S. KRUCKER[1], R. ABIAD[1], T. QUINN[1], P. BERG[1], M. HASHII[1],
R. STERLING[1], R. JACKSON[1], R. PRATT[1], R. D. CAMPBELL[1,10], D. MALONE[1],
D. LANDIS[1], C. P. BARRINGTON-LEIGH[1], S. SLASSI-SENNOU[1], C. CORK[5],
D. CLARK[3], D. AMATO[3], L. ORWIG[3], R. BOYLE[3], I. S. BANKS[3], K. SHIREY[3],
A. K. TOLBERT[3,16], D. ZARRO[3,26], F. SNOW[3], K. THOMSEN[4], R. HENNECK[4],
A. MCHEDLISHVILI[4], P. MING[4], M. FIVIAN[1,11], JOHN JORDAN[12],
RICHARD WANNER[12], JERRY CRUBB[12], J. PREBLE[12,13], M. MATRANGA[12,14],
A. BENZ[17], H. HUDSON[1], R. C. CANFIELD[18], G. D. HOLMAN[3], C. CRANNELL[3],
T. KOSUGI[19], A. G. EMSLIE[20], N. VILMER[21], J. C. BROWN[22], C. JOHNS-KRULL[23],
M. ASCHWANDEN[24], T. METCALF[24] and A. CONWAY[25]

[1]*Space Sciences Laboratory, University of California Berkeley, Berkeley, CA 94720-7450, U.S.A.*
[2]*Physics Department, University of California, Berkeley CA 94720–7300, U.S.A.*
[3]*NASA/Goddard Space Flight Center, Greenbelt, MD 20771, U.S.A.*
[4]*Paul Scherrer Institut (PSI), CH-5232 Villigen PSI, Switzerland*
[5]*Lawrence Berkeley National Laboratory, Berkeley, CA 94720, U.S.A.*
[6]*H. F. van Beek Consultancy (VBC), 3971 LB Driebergen, The Netherlands*
[7]*Tecomet, Woburn, MA 01801, now at Mikro Systems Inc., Charlottesville, VA, U.S.A.*
[8]*Ortec, Oak Ridge, TN 37831–0895*
[9]*University of Applied Sciences, CH-5210 Windisch, Switzerland*
[10]*Deceased*
[11]*Previously PSI*
[12]*Spectrum Astro, Gilbert, AZ 85233, U.S.A.*
[13]*SpaceWorks Inc., Carefree, AZ 85377–2014, U.S.A.*
[14]*The Charles Stark Draper Laboratory Inc., Cambridge, MA 02139–3563, U.S.A.*
[15]*Universtity of Maryland, College Park, MD 20742, U.S.A.*
[16]*Science Systems & Applications Inc. (SSAI), Lanham, MD 20771, U.S.A.*
[17]*ETHZ, Zürich CH-8092, Switzerland*
[18]*Montana State University, Bozeman, MT 59717, U.S.A.*
[19]*ISAS, Sagamihara City, Kanagawa Prefecture, Japan*
[20]*University of Alabama in Huntsville, Huntsville, AL 35899, U.S.A.*
[21]*Observatoire de Paris-Meudon, France*
[22]*University of Glasgow, Glasgow G128QW, Scotland, U.K.*
[23]*Rice University, Houston, TX 77005, U.S.A.*
[24]*Lockheed-Martin, Palo Alto, CA 94304, U.S.A.*
[25]*The Open University, Milton Keynes MK7 6AA, U.K.*
[26]*L-3 Communications, New York, NY 10016, U.S.A.*

Abstract. RHESSI is the sixth in the NASA line of Small Explorer (SMEX) missions and the first managed in the Principal Investigator mode, where the PI is responsible for all aspects of the mission except the launch vehicle. RHESSI is designed to investigate particle acceleration and energy release in solar flares, through imaging and spectroscopy of hard X-ray/gamma-ray continua emitted by energetic electrons, and of gamma-ray lines produced by energetic ions. The single instrument consists of an imager, made up of nine bi-grid rotating modulation collimators (RMCs), in front of a spectrometer with nine cryogenically-cooled germanium detectors (GeDs), one behind each RMC. It provides the first high-resolution hard X-ray imaging spectroscopy, the first high-resolution gamma-ray line spectroscopy, and the first imaging above 100 keV including the first imaging of gamma-ray lines. The spatial resolution is as fine as ~ 2.3 arc sec with a full-Sun ($\gtrsim 1°$) field of view, and the spectral resolution is $\sim 1-10$ keV FWHM over the energy range from soft X-rays (3 keV) to gamma-rays (17 MeV). An automated shutter system allows a wide dynamic range ($> 10^7$) of flare intensities to be handled without instrument saturation. Data for every photon is stored in a solid-state memory and telemetered to the ground, thus allowing for versatile data analysis keyed to specific science objectives. The spin-stabilized (~ 15 rpm) spacecraft is Sun-pointing to within $\sim 0.2°$ and operates autonomously. RHESSI was launched on 5 February 2002, into a nearly circular, 38° inclination, 600-km altitude orbit and began observations a week later. The mission is operated from Berkeley using a dedicated 11-m antenna for telemetry reception and command uplinks. All data and analysis software are made freely and immediately available to the scientific community.

1. Introduction

The processes of particle acceleration and impulsive energy release occur in active cosmic plasmas at diverse sites throughout the universe, ranging from planetary magnetospheres to active galactic nuclei. The understanding of these processes is a major goal of space physics and astrophysics, but we are just beginning to perceive the relevant basic physics. The Sun constitutes an unparalleled laboratory for investigating these processes. Its proximity allows measurements over the entire electromagnetic spectrum to be made on physically relevant scales. At the same time, the system as a whole can be studied, and escaping energetic particles and plasma can be sampled directly. Further, the complexity of solar magnetic fields and the solar atmosphere leads to a broad range of acceleration phenomena, mirroring the rich diversity of processes occurring on cosmic scales.

The primary scientific objective of RHESSI is to understand particle acceleration and explosive energy release in the magnetized plasmas at the Sun. The Sun is the most powerful particle accelerator in the solar system, accelerating ions up to tens of GeV and electrons to hundreds of MeV in solar flares and in fast coronal mass ejections (CMEs). Solar flares are the most powerful explosions, releasing up to $10^{32}-10^{33}$ ergs in 10^2-10^3 s. The flare-accelerated $\sim 10-100$ keV electrons (and sometimes $\gtrsim 1$ MeV nucleon ions) appear to contain a significant fraction, $\sim 10-50\%$, of this energy, indicating that the particle acceleration and energy release processes are intimately linked. How the Sun releases this energy, presumably stored in the magnetic fields of the corona, and how it rapidly accelerates electrons and ions with such high efficiency, and to such high energies, is presently unknown.
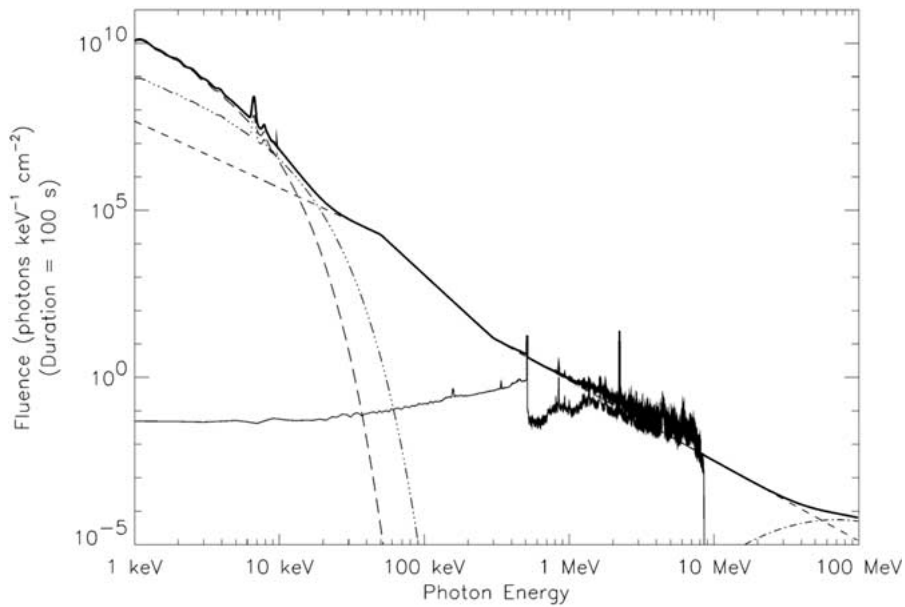
Figure 1. Composite X-ray/gamma-ray spectrum from 1 keV to 100 MeV for a large flare. At energies up to $\sim 10-30$ keV, emission from hot($\sim 10^7$ K) and 'superhot' ($\sim 3 \times 10^7$ K) thermal flare plasmas (the *two curves at the left*) dominate. Bremsstrahlung emission from energetic electrons produces the X-ray/gamma-ray continuum (*straight lines*) up to tens of MeV. Broad and narrow gamma-ray lines from nuclear interactions of energetic ions sometimes dominate the spectrum between ~ 1 to 7 MeV. Above a few tens of MeV the photons produced by the decay of pions (*curve at the right*) dominates. RHESSI observations cover almost four orders of magnitude in energy (3 keV to 17 MeV).

High-energy emissions are the most direct signature of the acceleration of electrons, protons and heavier ions in solar flares (Figure 1). Accelerated electrons colliding with the ambient solar atmosphere produce bremsstrahlung hard X-ray and gamma-ray continuum emission, while nuclear collisions of energetic ions result in a complex spectrum of narrow and broad gamma-ray lines. Hot (million-degrees) thermal flare plasmas also emit bremsstrahlung X-rays. RHESSI is designed to provide high resolution imaging and spectroscopy of all these emissions, from soft X-rays (3 keV) to gamma-rays (17 MeV).

These emissions are accompanied by longer wavelength emissions, and sometimes by escaping energetic particles. Their observation by the fleet of spacecraft (Solar and Heliospheric Observatory (SOHO), WIND, Advance Composition Explorer (ACE), *Ulysses*, Transition Region And Coronal Explorer (TRACE), Geostationary Operational Environmental Satellite Project (GOES), Solar Anomalous and Magnetospheric Particle Explorer (SAMPEX), etc.) already in place, and by ground-based instruments, provides the crucial information on the context in which the high energy processes occur.

RHESSI is the first Small Explorer mission carried out in the 'Principal Investigator-mode', where the PI and team are responsible for all aspects of the

mission except providing the launch vehicle. This includes developing, integrating, and testing the instrument and spacecraft; providing launch support, telemetry downlink and command uplink, mission and science operations, data processing and distribution; analyzing and archiving the data, and disseminating the results.

The RHESSI mission was selected by NASA in October 1997, with a very aggressive development schedule aimed at a launch in July 2000, near the predicted peak of the ~ 11-year solar activity cycle. During environmental testing of the integrated spacecraft at the Jet Propulsion Laboratory in March 2000, however, a malfunction in the shake table subjected RHESSI to a vibration level of > 25 G rather than the requested 2 G, resulting in extensive damage to both the instrument and spacecraft. At about this time the failure of a Mars orbiting mission and then a Mars lander led NASA to institute a policy of additional external 'Red Team' reviews. Even with all the extra effort involved in these reviews and the implementation of their recommendations, the instrument and spacecraft were repaired, re-integrated, and re-tested in time for a launch at the end of 2000.

A problem was then discovered on the three-stage solid-propellant Pegasus-XL launch vehicle, and fixing that problem delayed the launch to March 2001, and again to June 2001. In April 2001, the RHESSI spacecraft was integrated with the Pegasus-XL at Orbital Science Corporation's facilities in the Western Test Range, and in early June it was carried underneath an L-1011 aircraft to the Eastern Test Range at Kennedy Space Center. One week before the planned RHESSI launch, NASA attempted a test flight of the prototype X-43 aerospace plane. The modified Pegasus first stage used for launch failed and the X-43 had to be destroyed. This led to a series of further delays while the cause of the failure was investigated. Finally, on 5 February 2002, the RHESSI satellite was launched by the Pegasus-XL, following its release from the L-1011 at $\sim 40\,000$ feet altitude over the Atlantic Ocean. A near perfect, 38° inclination, 600 km altitude circular orbit was achieved.

The mission was renamed from HESSI to RHESSI after launch to honor Dr Reuven Ramaty, a distinguished theoretical high-energy astrophysicist and solar physicist working at Goddard Space Flight Center (GSFC). Dr Ramaty developed much of the theoretical framework for solar gamma-ray line spectroscopy, and he was a Co-I and a strong advocate of RHESSI. He passed away in March 2001, eight months after the planned launch date, but 11 months prior to the actual launch. He is the first NASA scientist to have a space mission named after him.

2. Scientific Objectives and Design Considerations

2.1. ACCELERATION OF ELECTRONS

Bursts of bremsstrahlung hard X-rays ($\gtrsim 20$ keV), emitted by accelerated electrons colliding with the ambient solar atmosphere, are the most common signature of the impulsive phase of a solar flare (Figure 2). Provided the electron energy E_e is much
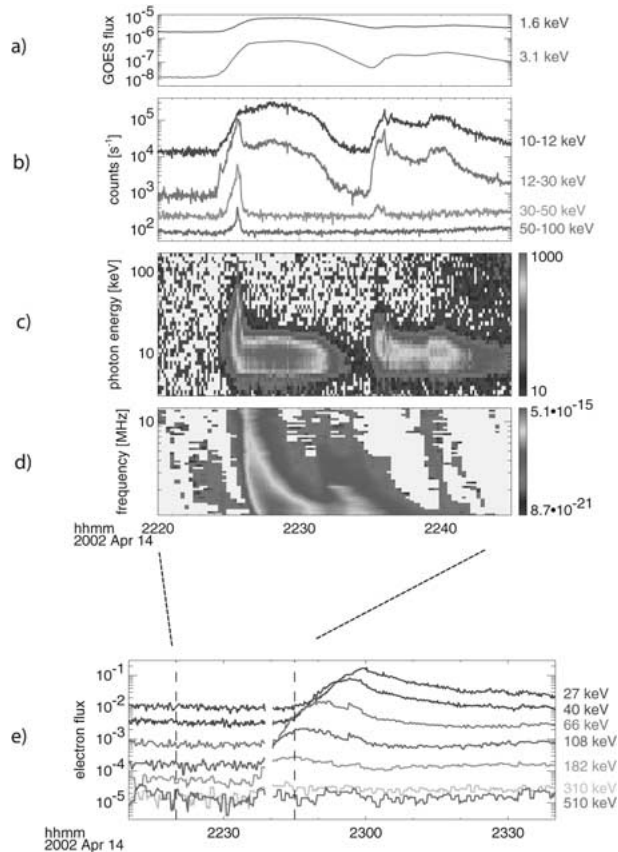
Figure 2. [See CD-ROM for color version]. Time profile of X-ray fluxes from GOES (a) and RHESSI (b); counts are multiplied by factors of 8, 50, and 500, for the 30–50 keV, 12–30 keV, and 10–12 keV channels, respectively). The next two panels show spectrograms of (c) the RHESSI counts in 20 logarithmic energy channels, and of (d) 1–14 MHz radio emission detected by the WIND spacecraft (Bougeret *et al.*, 1995). The solar flare with hard X-ray peak at ∼ 22:26 UT is accompanied by a type III solar radio burst, produced by energetic electrons escaping the Sun. The (e) bottom panel (longer time interval) shows the energetic electrons arriving at WIND at 1 AU (Lin *et al.*, 1995), with the faster electrons arriving first, consistent with an impulsive injection of the electrons from the Sun at the time of the X-ray peak.

greater than the average thermal energy, kT, of the ambient gas, essentially all of the electron energy will be lost to Coulomb collisions, with only a tiny fraction (∼ 10^{-5}) lost to bremsstrahlung. For this non-thermal situation, the hard X-ray fluxes observed in many flares indicate that the energy in accelerated > 20 keV electrons must be comparable to the total flare radiative and mechanical output (Lin and Hudson, 1976). Thus, the acceleration of electrons to tens of keV may be the most direct consequence of the basic flare-energy release process.

High-resolution hard X-ray imaging spectroscopy is the key to understanding the electron acceleration and energy release processes in solar flares. High-spectral-
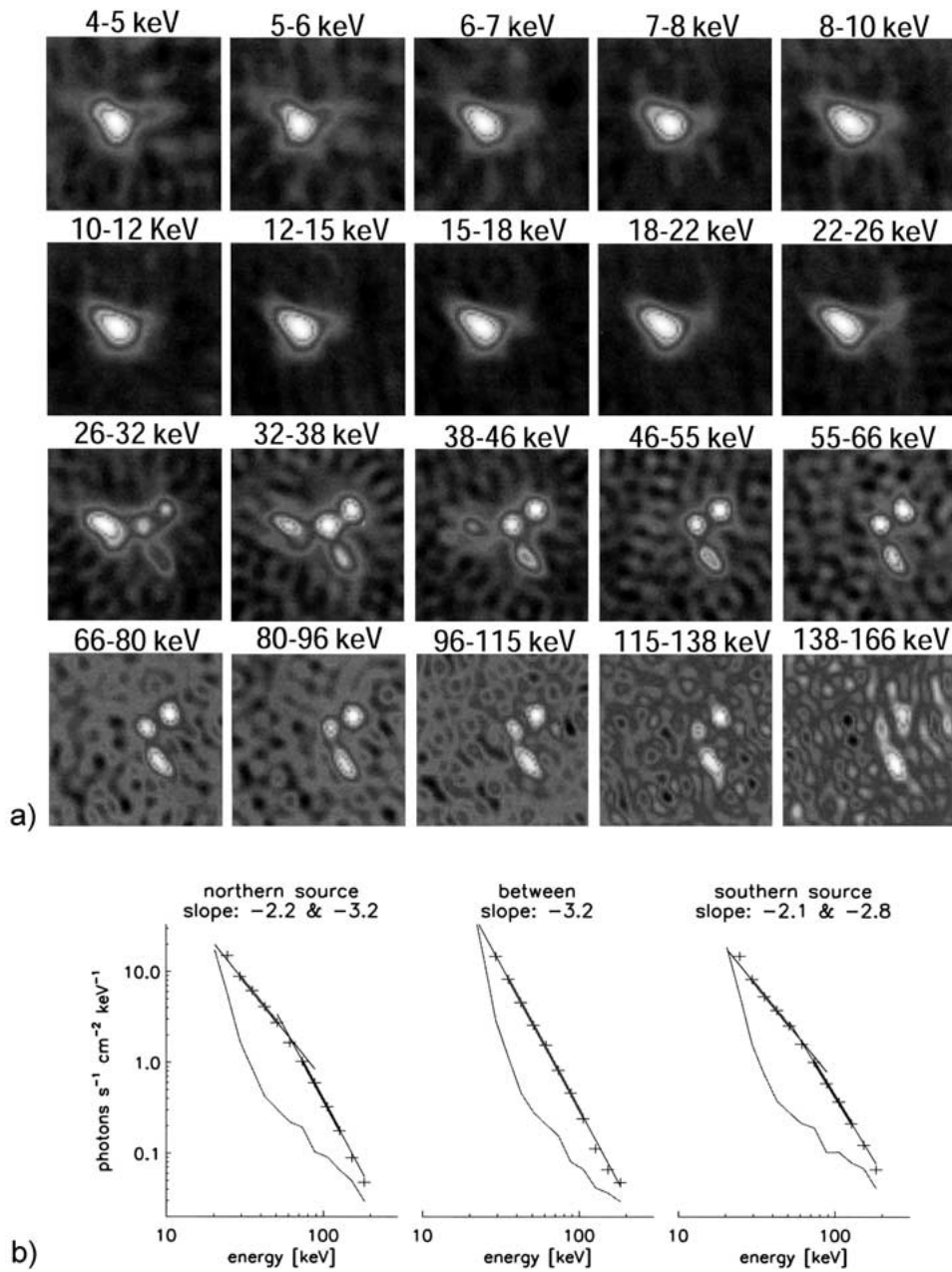
resolution measurements of the solar flare hard X-ray spectrum can be directly inverted to obtain the detailed spectrum of the parent X-ray-producing electrons (Johns and Lin, 1992). RHESSI is designed to provide imaging spectroscopy – the photon spectrum is obtained in each spatial element (Figure 3) as a function of time. In principle, this spectrum provides detailed information on $N(E, \mathbf{r}, t)$, the X-ray producing electron number density, as a function of energy (E), position ($\mathbf{r}$), and time (t). With information from context observations on the ambient density, temperature, magnetic field strength and topology, the electron loss processes can be directly evaluated to determine whether the X-ray emission is thermal or non thermal. By using a spatially dependent continuity equation, including loss processes, the spatially and temporally resolved accelerated electron source distribution, $F(E, \mathbf{r}, t)$, can be inferred. Then, detailed quantitative models of the acceleration, energy release, and energy propagation processes can be constructed and tested.

RHESSI is designed to provide spatial (Figure 4(b)) and temporal resolution commensurate with the spatial and temporal scales for the accelerated electrons to lose their energy in the lower corona and upper chromosphere (ambient densities below $\sim 10^{12}$ cm^{-3}). To resolve the very steep thermal spectra and determine the lower energy limit of the non-thermal spectrum (critical to determining the energy content in fast electrons), ~ 1 keV spectral resolution (Figure 4(a)) is needed. The energy range should extend low enough so the thermal–nonthermal transition can be determined, and as high as practical, but certainly up to relativistic energies where a different acceleration process may be operating. Finally, high sensitivity is required to detect microflares (which may be important for coronal heating), and very wide dynamic range is required to make measurements in the largest flares without saturation.

2.2. ACCELERATION OF IONS

Near the Sun, nuclear collisions of accelerated ions with the ambient solar atmosphere result in a rich spectrum (Figure 1) of gamma-ray lines (Ramaty and Murphy, 1987; Chupp, 1990, Share and Murphy, 1995). Energetic protons and alpha-particles colliding with carbon and heavier nuclei produce narrow de-excitation lines (widths of $\sim$ few keV to ~ 100 keV), while energetic heavy nuclei colliding with ambient hydrogen and helium produce much broader lines (widths of hundreds of keV to an MeV). Neutron capture on hydrogen and positron annihilation produce delayed narrow lines, at 2.223 MeV and 0.511 MeV, respectively.

The bulk of the gamma-ray line emission is produced by ions with energies of 10–100 MeV nucleon that contain only a small fraction of the energy in the $\gtrsim 20$ keV electrons. However, systematic study of SMM gamma-ray line flares (Share and Murphy, 1995) showed that the 1.634 MeV ^{20}Ne line is enhanced relative to other lines. Because the cross section for ^{20}Ne has an unusually low energy threshold (~ 2.5 MeV), this effect appears to be due to large fluxes of low-energy

Figure 3. [See CD-ROM for color version]. (a) Imaging of the July 23, 2002, X4.8 solar flare in 20 energy bands, from 1 keV wide bins at 4 keV, to 28 keV wide bins (for enough counts to image) at 138 keV, illustrating the changes in sources as a function of energy, from a single dominant elongated source at energies below ~ 30 keV to three sources above ~ 40 keV. The images are 64 arc sec on a side; the lower left corner is just at the southeast limb of the Sun. (b) The energy spectra of the three dominant sources at energies above ~ 40 keV, showing that the spectra are similar for the north and south sources but quite different for the source in between. The *dashed lines* indicate background.
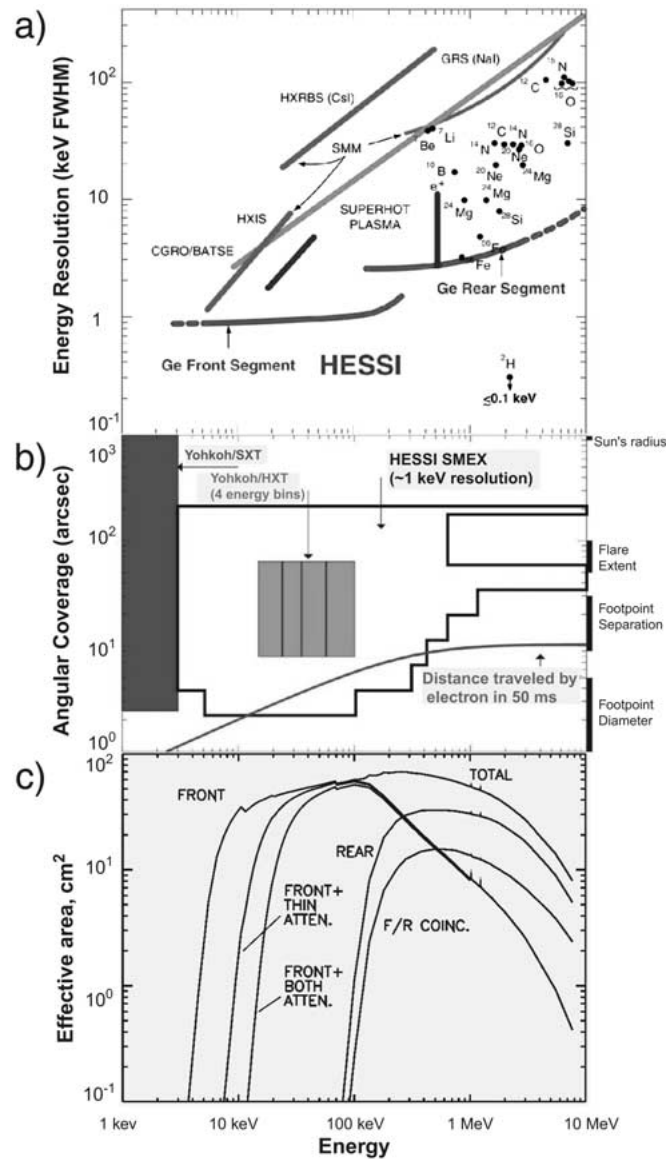
Figure 4. [See CD-ROM for color version]. (a) RHESSI's Full Width at Half Maximum (FWHM) energy resolution (*lower curves*), compared with previous instruments (*upper lines*). The *dots* are the expected FWHM widths of the predicted gamma-ray lines, and the *vertical line* the range of widths (temperature and density dependent) for the positron annihilation line. The *short diagonal line* shows the resolution needed to resolve the steep 'superhot thermal' emission. (b) RHESSI's angular resolution versus energy, compared to *Yohkoh* Soft X-ray Telescope (SXT) (*left*) and Hard X-ray Telescope (HXT) (*center*). RHESSI has ∼ 1–10 keV energy resolution over this energy range and can image up to 17 MeV, while HXT had four broad energy channels from 15 to 100 keV. (c) RHESSI's effective (photopeak) area as a function of energy for solar X-rays/gamma-rays. The *three curves to the left* show the effect on the front segment response (summed over all nine detectors) of no attenuators, thin attenuator, or both thick and thin attenuator inserted over the detectors. The *curves to the right* show the effective area for the rear segment, and for photons that leave energy in both the front and rear segment of the detectors (F/R coincidence).

ions with total energy content often comparable to that of the accelerated electrons (Ramaty *et al.*, 1995; Emslie *et al.*, 1997).

RHESSI is designed to probe ion acceleration with the first high-resolution spectroscopy of solar flare gamma-ray lines (Figure 4(a)), giving the first detailed line shapes, which depend on the angular distribution of the interacting accelerated ions. The shape of the 0.511 MeV positron annihilation line gives information about the density and temperature of the ambient medium since the positrons slow down before annihilating. The high resolution enables closely spaced lines to be separated, particularly important around 1 MeV, where several lines are produced by accelerated ^{3}He. Their detection would test whether gamma-ray flares and impulsive, ^{3}He-rich solar energetic particle events have a common origin (Ramaty *et al.*, 1993).

RHESSI is also designed to image solar flare gamma-ray lines (Figure 4(b)), thus providing the first information on the locations of energetic heavy ions and protons and their secondary neutrons and positrons, to compare with the location of the energetic electrons. The instrument's high spectral resolution allows imaging in narrow gamma-ray lines, such as the 2.223 MeV neutron capture line, where line counts dominate over the background. The continuum above ~ 1 MeV (especially 4–7 MeV) is often dominated by the broad lines from accelerated heavy ($Z > 2$) ions, and can be imaged to locate them. In a very large gamma-ray line flare with good statistics, the > 2.5 MeV protons might be located by imaging the ^{20}Ne de-excitation line.

2.3. NON-SOLAR SCIENCE

Although designed as a solar instrument, RHESSI's lack of shielding around the detectors (to minimize weight) makes it an effective high-spectral-resolution ($\sim$ keV FWHM), wide-field-of-view hard X-ray/gamma-ray all-sky monitor, with ~ 150 cm^2 collecting area. The spacecraft's rotation produces many detector/detector occultations per minute, and two brief Earth occultation/deoccultations occur per orbit (Harmon *et al.*, 1992; Zhang *et al.*, 1993), allowing localization of transients (black-hole X-ray novae, Be/neutron star binary outbursts, etc.) and steady sources. RHESSI is able to resolve cyclotron absorption features from bright transients such as A0535+26, search for line features in gamma-ray bursts, and study the Galactic positron annihilation and ^{26}Al decay lines from nucleosynthesis in supernovae and massive stellar systems on large angular scales. RHESSI can image the Crab Nebula once a year (when it approaches within 1.6° of the Sun), with unprecedented spatial (2.3 arc sec) and energy (~ 1 keV) resolution in hard X-rays. RHESSI also provides high spectral and temporal resolution measurements of terrestrial X-ray/gamma-ray continuum emissions from electron precipitation, of terrestrial gamma-ray line emission from the impact of cosmic rays and solar energetic particles, and of gamma-ray bursts associated with lightning (Fishman *et al.*, 1994).

3. Instrument

The RHESSI scientific objectives are achieved with high-resolution imaging spectroscopy observations from soft X-rays to gamma-rays, utilizing a single instrument consisting of an Imaging System, a Spectrometer, and the Instrument Data Processing Unit (IDPU) containing the instrument electronics. An instrument schematic is shown in Figure 5 and the specifications are given in Table Ia. The Imaging System is made up of nine Rotating Modulation Collimators (RMCs), each consisting of a pair of widely separated grids mounted on a rotating spacecraft. Pointing information is provided by the Solar Aspect System (SAS) and redundant Roll Angle Systems (RASs). The Spectrometer has nine segmented germanium detectors (GeDs), one behind each RMC, to detect photons from 3 keV to 17 MeV. The GeDs are cooled to $\lesssim 75$ K by a space-qualified long-life mechanical cryocooler, to achieve the highest spectral resolution (Figure 4(b)) of any presently available gamma-ray detector. As the spacecraft rotates, the RMCs convert the spatial information from the source into temporal modulation of the photon counting rates of the GeDs. The instrument electronics amplify, shape, and digitize the GeD signals, provide low-voltage power and GeD high voltage, format the data, and interface to the spacecraft electronics.

The energy and arrival time of every photon, together with aspect data, are recorded in the spacecraft's on-board 4-Gbyte solid-state memory (sized to hold all the data from the largest flare) and automatically telemetered within 48 hours. With these data, the X-ray/gamma-ray images can be reconstructed on the ground (see Figure 3). The instrument's $\sim 1°$ field of view is much wider than the $\sim 0.5°$ solar diameter, so all flares are detected, and pointing can be automated.

3.1. Imaging system

A detailed description of the RHESSI imaging technique is given in Hurford *et al.* (2002). At hard X-ray and gamma-ray energies, unlike soft X-rays, EUV, and longer wavelength emissions, focusing optics are not feasible. The only viable method of obtaining arcsecond-class images in hard X-rays and gamma-rays within the Small Explorer constraints is with Fourier-transform imaging, similar to that used in the pioneering *Hinotori* rotating modulation collimator (Makishima *et al.*, 1977) and *Yohkoh* Hard X-ray Telescope (HXT) (Kosugi *et al.*, 1991). RHESSI uses nine collimators, each made up of a pair of widely separated grids. Each grid is a planar array of equally-spaced, X-ray-opaque slats separated by transparent slits (Figure 6). The slits of each pair of grids are parallel to each other and their pitches (p) are identical, so that the transmission through the grid pair depends on the direction of the incident X-rays. For slits and slats of equal width, the transmission is modulated from zero to 50% and back to zero for a change in source angle to collimator axis (orthogonal to the slits) of p/L where L is the separation between grids. The angular resolution is then defined as $p/(2L)$.

TABLE I
RHESSI characteristics.

Ia. Instrument characteristics:

Energy range	3 keV to 17 MeV
Energy resolution (FWHM)	$\lesssim 1$ keV at 3 keV, increasing to ~ 5 keV at 5 MeV
Angular resolution	2.3 arc sec to 100 keV, 7 arc sec to 400 keV, 36 arc sec to 15 MeV
Temporal resolution	2 s for detailed image, tens of ms for basic image
Field of view	full Sun ($\sim 1°$)
Effective area (photopeak)	$\sim 10^{-3}$ cm^2 at 3 keV, ~ 32 cm^2 at 10 keV (with attenuators out), ~ 60 cm^2 at 100 keV, ~ 15 cm^2 at 5 MeV
Detectors	9 germanium detectors (7.1-cm dia. $\times$ 8.5 cm), cooled to < 75 K with Stirling-cycle mechanical cooler
Imager	9 pairs of grids, with pitches from 34 microns to 2.75 mm, and 1.55-m grid separation
Aspect system	Solar Aspect System: Sun center to < 1 arc sec Roll Angle System: roll to ~ 1 arc min
Number of flares expected	~ 1000 imaged to > 100 keV $\sim$ tens with spectroscopy to ~ 10 MeV

Ib. Spacecraft characteristics:

Mass	Total 291.1 kg, instrument 130.8 kg
Power	Total 220.4 W, instrument 142.3 W
Size	1.18 m diameter, 2.06 m height, 5.74 m tip-to-tip with solar panels deployed
Telemetry	4 Mbps, downlink, 2 kbps command uplink
On-board storage	4 Gbyte solid state memory
Attitude	15 rpm spin rate, pointing to $0.2°$ of Sun center

Ic. Mission characteristics:

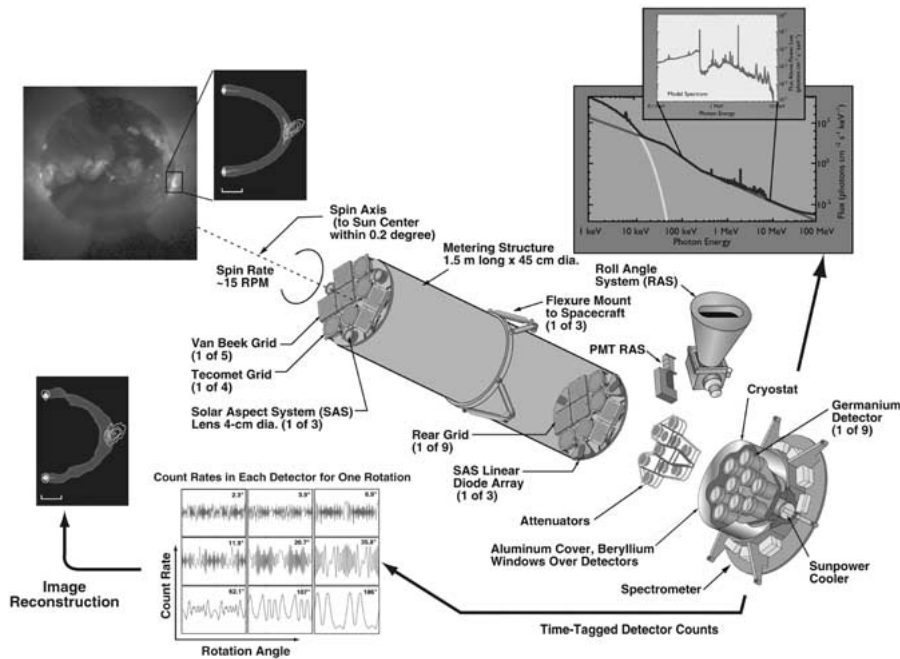|	
Launch date	5 February 2002
Launch vehicle	Pegasus XL
Orbit	$38°$ inclination, 600 km altitude apogee, 586 km perigee
Nominal mission lifetime	2 years, 3rd year highly desirable

Figure 5. [See CD-ROM for color version]. Schematic of the RHESSI instrument illustrating the imaging spectroscopy. X-rays and gamma-rays from the Sun (*upper left*) pass through the slits of the front and rear grids of each of the nine grid pairs to reach the germanium detector. As the spacecraft rotates the detector count rates are temporally modulated (*lower left*). These modulations can be analyzed to reconstruct the image. The germanium detectors are cryogenically cooled to provide high spectral resolution capable of resolving narrow gamma-ray lines and steep solar continuum spectra (*upper right*). The attenuators are inserted automatically when the count rate approaches saturation. The SAS, RAS and PMTRAS provide solar pointing and roll aspect information.

For RHESSI, the transmission of the source photons through the grids is modulated by mounting the instrument on a rotating spacecraft. The X-ray/gamma-ray detector behind the collimator records the arrival time and energy of individual photons, allowing the modulated counting rate to be determined as a function of rotation angle. Note that the detector does not need to have any spatial resolution and hence can be optimized for high sensitivity and energy resolution.

For a parallel incident beam, the modulated waveform generated by a smoothly rotating spacecraft has a distinctive quasi-triangular shape locally. The amplitude is proportional to the intensity of the beam, and the phase and frequency depend on the direction of incidence. For complex sources, and over small rotation angles, the amplitude and phase of the waveform provide a direct measurement of a single Fourier component of the angular distribution of the source (e.g., Prince *et al.*, 1988). Different Fourier components are measured at different rotation angles and with grids of different pitches. For RHESSI, the separation between grids in each RMC is L = 1.55 m and the grid pitches range from $p = 34$ μm to 2.75 mm in steps
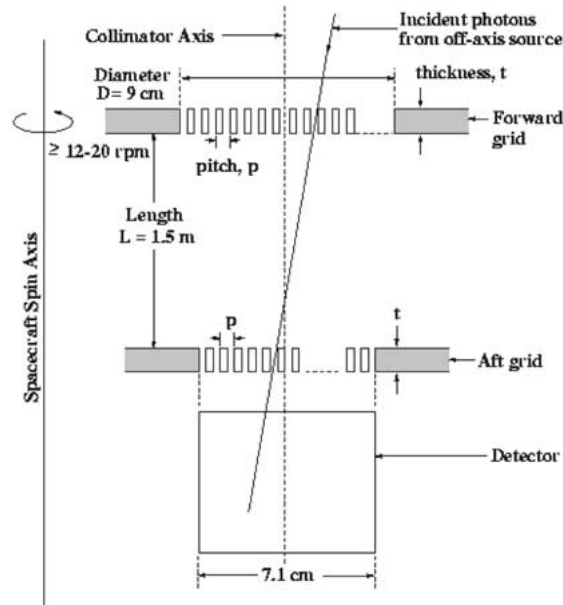
Figure 6. Schematic showing the parameters that define the imaging capability.

of $\sqrt{3}$. This provides angular resolutions spaced logarithmically from 2.3 arc sec to $\gtrsim 3$ arc min, allowing sources to be imaged over a wide range of angular scales. Diffuse sources larger than 3 arc min are not imaged but full spectroscopic information is still obtained. Multiple smaller sources are imaged regardless of their separation.

In a half rotation (2 s), the nine RMCs measure amplitudes and phases of ~ 1100 Fourier components for a typical source location, compared to 32 Fourier components for the *Yohkoh* HXT, so that far more complex flare images can be resolved. Although one half rotation is required to measure a full set of Fourier components, the measurement of each component takes only a single modulation cycle, which can be as short as 1.3 ms for the finest grids. Thus, when count rates are sufficiently high, crude images (from about ten Fourier components) can be obtained, in principle, on timescales of tens of milliseconds.

Changing the separation (L) between grids or displacing the grids parallel to the slits has little effect on imaging performance. A relative displacement perpendicular to the slits affects the phase but not the amplitude of modulation. Any such displacement will be accurately monitored by the SAS, and can be fully compensated for in the image reconstruction process. The critical alignment requirement is associated with the rotation or twist of one grid with respect to the other about the line of sight to the source. A relative twist of p/D ($D =$ diameter of grid) reduces the modulated amplitude almost to zero. Thus, the grid pairs must be well aligned in twist throughout the mission. For the finest grids (2.3 arc sec resolution) a 1-arc min alignment is needed. Thus, HESSI can achieve arc-sec-quality images with

an instrument having only arc-min alignment requirements. To minimize twist, the grids are aligned and mounted precisely on grid trays which are attached to opposite ends of a graphite-epoxy support tube.

3.1.1. *Grids*

The main challenges in fabricating the RHESSI grids were: (i) the extremely fine slit and slat widths (20 and 14 microns for 34 micron pitch) required for the finest grid, (ii) the high (50 : 1) aspect ratio of the slit width to grid thickness for maximum absorption consistent with a $\sim 1°$ field of view, and (iii) the fine tolerance on the relative pitches of the two grids in each pair (< 1 part in 20 000 for the finest grid pair). Tecomet, Inc., fabricated the four finest grid pairs (plus a third spare grid) using a foil stacking method in which thin sheets of metal were photo-etched and precision stacked with epoxy bonding to produce a solid structure (Figure 7(a), left). Tungsten was used for all of the grids except for the finest; grid pair 1 (Figure 7(b)) was made of molybdenum (sufficiently thin tungsten sheets were not available then), resulting in a maximum energy for modulation of ~ 100 keV, rather than ~ 200 keV had it been tungsten. The five coarsest grid pairs were made by van Beek Consultancy in The Netherlands using tungsten blades packed together side by side with spacers in between (Figure 7(a), right) to give the required, pitch, slit width, and grid thickness. The thickest grids, No. 6 (Figure 7(c)) and 9 (1.85 and 3 cm thick) were designed to modulate gamma-rays up to 17 MeV (Figure 4(b)).

All the grids were fully characterized at GSFC both optically and using X-rays. Optical images were taken at high magnification of the front and rear of each grid using a customized facility. Each grid was mounted on an XY table with laser readout, and measurements of the pitch, phase, and orientation of the slits in each grid were obtained with micron positional accuracy. A separate X-ray characterization facility determined the average X-ray transmission of each flight grid as a function of photon energy and angle from grid normal. In addition, the variation of this transmission across the full area of each grid was measured with ~ 1-cm resolution.

All grids were also fully flight qualified at GSFC by vibration testing and thermal cycling to GEVS (General Environmental Verification Specification) standards. The grids were then transported to Paul Scherrer Institut (PSI) in Switzerland where they were mounted and aligned on the front and rear end trays. Precision coordinate measurement machines were used to establish and verify the correct alignment of each grid pair, so that in the final assembly the slits of the front and rear grids of each pair would be parallel to within the very strict tolerances required for modulation of the incident photon flux.

After assembly of the trays onto the imager tube at PSI, an end-to-end check on the grid alignments was carried out. Since an X-ray beam parallel to $\lesssim 1$ arc sec could not be obtained, a radioactive ^{109}Cd source was placed behind the spare grid for each pair, to provide a series of diverging fan beams of 22 keV X-rays. By moving this source/grid while maintaining an appropriate distance from the grid
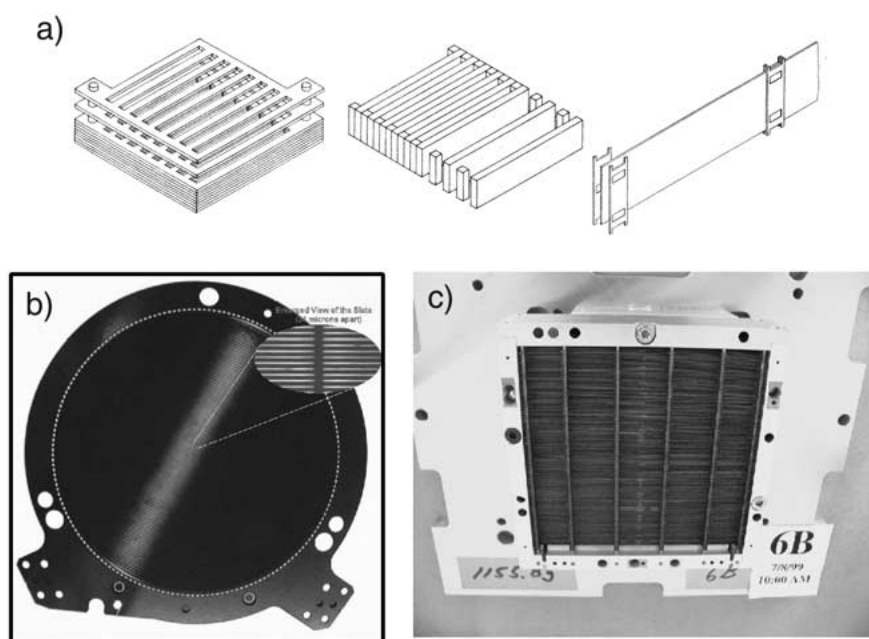
Figure 7. [See CD-ROM for color version]. (a) Schematic of the two grid fabrication processes: left, stacking etched foils and epoxying them to obtain the required thickness; middle and right, packing vertical blades with spacers in between. (b) Photograph of a grid No. 1 showing the slits and bridges in the insert. (c) Photograph of flight grid No. 6.

pair, a modulation in transmission would be detected providing that the two grids of that pair were correctly aligned. This test was carried out on all but the two coarsest grid pairs – their alignments could be checked visually.

For long-term monitoring of the grid alignment through all testing and environmental qualification prior to launch, an optical twist monitoring system (TMS) was used repeatedly. This system relied on optical photodiodes mounted behind pinholes in the rims of the rear grids. The light from these photodiodes passed through annuli mounted in the front grids in such a way that the diffracted beams from any one grid pair converged onto a Charge Couple Device (CCD) camera mounted at the appropriate distance in front of the telescope assembly. The positions of the converging beams as determined from the images provided an accurate measure of any change in the relative twist of the front and rear grids of a each pair. In this way, the correct alignment of even the finest grid pair could be verified up to launch. No significant change in alignment was ever measured except after the vibration accident at Jet Propulsion Laboratory (JPL), when the front grid No. 6 was hit and moved on its mount. The complete imaging telescope system was shipped back to PSI, a new mount installed for the front grid 6, and all grid alignments were rechecked and verified, including repeating the TMS check.

3.1.2. *Aspect Systems*

The ability to make arc-sec-quality images and accurately co-align the images with other solar observations, depends on knowing the orientation of the collimators with respect to the direction to the Sun at all times. This essential aspect information is obtained with the Solar Aspect System (SAS), which provides pitch and yaw measurements relative to the solar limbs to arcsecond accuracy on time scales of tens of ms, and two redundant Roll Angle Systems – a CCD-based version (CCD RAS) and a photomultiplier-based version (PMT RAS) – that each provide the roll angle to arc min accuracy several times per rotation with respect to the fixed stars. Full details of these systems are given by Zehnder *et al.* (2002) for the SAS and CCD RAS and by Hurford and Curtis (2002) for the PMTRAS.

3.1.3. *Solar Aspect System (SAS)*

The Solar Aspect System (SAS) provides (1) high-resolution, high-bandwidth aspect information for image reconstruction, (2) monitoring of the relative twist of the two grid trays, and (3) full-Sun white-light images, on occasion, for co-alignment with ground-based images. It consists of three identical lens-filter assemblies mounted on the forward grid tray to form full-Sun images on three 2048×13-μm linear diode arrays mounted on the rear grid tray. Simultaneous exposures of three chords of the focused solar images are made every 10 ms by each of the arrays. A digital threshold algorithm is used to select four (or more, commandable) pixels that span each solar limb for inclusion in the telemetry. These digitized pixel outputs allow six precise locations of the solar limb to be obtained on the ground by interpolation, thus providing knowledge of Sun center in pitch and yaw to 1.5 arc sec per readout (3σ).

3.1.4. *Roll Angle System (RAS)*

For image reconstruction on the ground (no impact on real-time spacecraft operations), knowledge of relative roll is required at all times to 3 arc min (3σ). Since all sources of torque on the spacecraft are weak, the required information can be obtained with a star scanner that samples the roll orientation at least once per rotation. Interpolation between measurements allows the roll orientation to be determined at intermediate times with the required accuracy. The CCD RAS consists of a CCD array and electronics behind an $f/1.0$, 50-mm lens. A sunshade limits the field of view so that a 30° band is swept out across the sky at 15° to orthogonal to the spin axis. As the spacecraft rotates, each detected star generates a brief spike in the output of one or two pixels, whose timing defines the roll orientation. For $+2$ magnitude stars, the detection signal-to-noise is $15:1$. Allowing for Earth occultation and the recovery time from anticipated earthshine saturation, at least one (and typically seven) such star(s) will be detected each rotation throughout the mission. Measurements of only one star, averaged over a minute, allow the roll angle to be determined to 2.7 arc min (3σ).
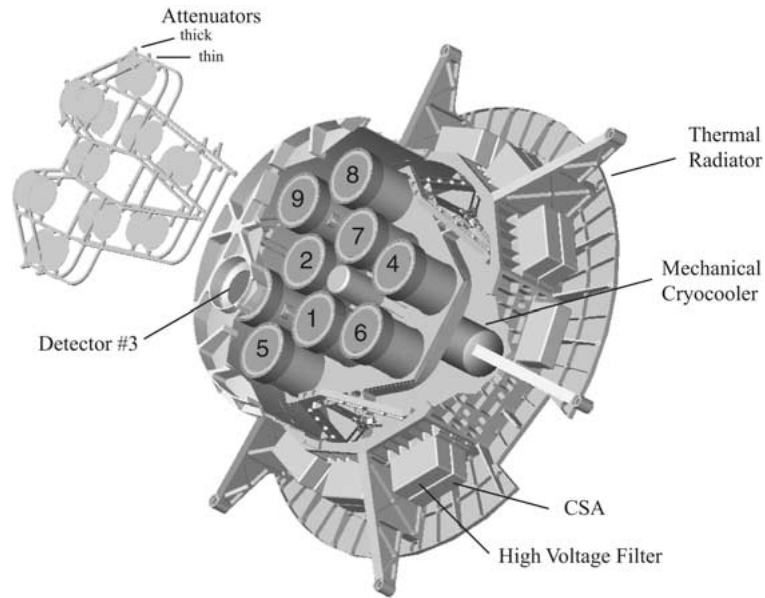
Figure 8. [See CD-ROM for color version]. A cutaway of the Spectrometer, showing the location of the germanium detectors under each grid (by number). The Sunpower Stirling-cycle mechanical cooler is below the cold plate holding the detectors. The thermal radiator faces anti-sunward to reject the heat of the cryocooler. The attenuators are automatically moved in when the counting rate exceeds thresholds (commandable from the ground).

The Aspect Data Processor (ADP) receives the data from the SAS and RAS, performs on-line processing. The PMTRAS, consisting of a photomultiplier (PMT) behind a slit to scan for bright stars, was included for redundancy.

3.2. SPECTROMETER

Figure 8 shows a cutaway of the Spectrometer, described in detail in Smith *et al.* (2002). The RHESSI germanium detector (GeD) design provides energy coverage from 3 keV to 17 MeV with a single mechanically robust detector. The largest, readily available, hyperpure (n-type) coaxial germanium material (7.1-cm diam $\times$ 8.5-cm long) was used. The inner electrode is segmented into two contacts that collect charge from two electrically independent detector segments, to provide the equivalent of a ~ 1.5-cm thick planar GeD in front of a ~ 7 cm thick coaxial GeD. The top and curved outer surfaces are implanted with a thin (0.3 micron) boron layer to provide a surface transparent down to 3 keV X-rays. With advanced Field Effect Transistors (FETs) and state-of-the-art electronics, the front segments achieve a 3-keV energy threshold.

The front segment thickness is chosen to stop photons up to ~ 250 keV (Figure 4(c)), where photoelectric absorption dominates, while minimizing the active volume for background. Front-incident photons that Compton-scatter, and back-

ground photons or particles entering from the rear, are rejected by anticoincidence with the rear segment; a passive, graded-Z (Pb, Cu, Sn) ring around the front segment absorbs hard X-rays incident from the side, to provide the low background of a phoswich-type scintillation detector. Photons with energies from ~ 250 keV to 17 MeV, including all nuclear gamma-ray lines, stop primarily in the thick rear segment alone, with smaller fractions stopping in the front segment, depositing energy in both the front and rear segments, or in two or more GeDs. All these modes contribute to the total photopeak efficiency (Figure 4(c)).

The intense hard X-ray fluxes that usually accompany large gamma-ray line flares are absorbed by the front segment, so the rear segment will always count at moderate rates. This is essential for gamma-ray line measurements where optimal spectral resolution and low dead time are desired. To accommodate the large dynamic range ($\sim 10^7$) in soft X-ray flux from microflares to very large flares, two sets of aluminum disk attenuators (also called shutters) can be moved in front of the GeDs to absorb low energy (see Figure 4(c)) photons. These attenuators are inserted automatically by heating temperature-sensitive Shape Memory Alloy (SMA) actuators when the count rate increases above pre-set values. The attenuation stays in for a fixed duration currently (~ 5 min), but programmable and then are removed. The cycle repeats as long as the rates stay high.

The GeDs in their modules are mounted on an aluminum cold plate suspended on fiberglass straps to reduce thermal conduction. This is surrounded by multi-layer radiation shields and enclosed in an evacuated cryostat. The cryostat's curved sidewall is ribbed thin-wall aluminum near the GeDs to provide ~ 20 keV threshold for non-solar X-ray/gamma-rays incident on the side.

The GeDs are cooled on-orbit by a single Sunpower Inc. M77B single-stage, counterbalanced, Stirling-cycle cryocooler. The interface is a flexible aluminum/sapphire cold finger designed to minimize coupling of microphonics into the GeDs and to allow a structured cooldown to avoid condensation of contaminants onto the GeDs. The cryocooler uses a gas bearing/flexure system to prevent contact between moving parts, and a moving-magnet motor to eliminate flexible motor leads. This cooler provides up to 4 W of cooling at 77 K, at an input power of 100 W. The cryocooler is mounted in an external cavity between the radiator and cryostat to minimize losses in the heat rejection path. The anti-Sun facing heat rejection radiator (76 cm diameter) is thermally coupled to the cryostat housing to provide a large thermal mass. The equilibrium radiator temperature is in the range of $-15\,°C$ to $-30\,°C$.

Radiation damage of the GeDs is of concern since RHESSI passes through the South Atlantic Anomaly (SAA) on about 5 orbits a day. Bombardment by high energy SAA protons produces traps in the GeDs which degrade the spectral resolution with time. The Spectrometer is designed with the capability to anneal the GeDs, by heating them up to $\sim 100\,°C$, to recover the resolution. This is not expected to be needed within the nominal two-year mission lifetime.
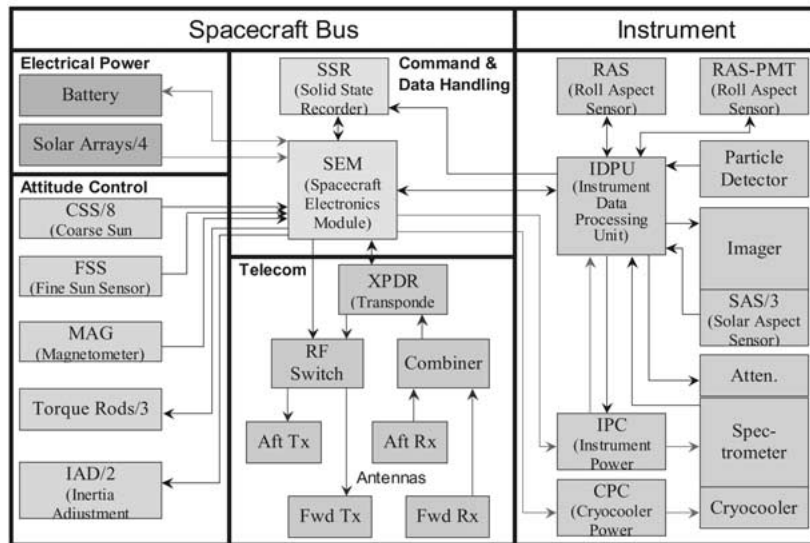
Figure 9. Block diagram for the RHESSI spacecraft bus (*left*) and the instrument (*right*).

3.3. INSTRUMENT ELECTRONICS

Each GeD is biased at between 4 and 5 kV by a separate adjustable high-voltage power supply. Photons interacting in a GeD generate charge pulses, which are collected and amplified by a transistor-reset Charge Sensitive Amplifier (CSA) with an advanced 4-terminal type FET to provide the best resolution and high-count rate performance. The CSAs and the high voltage filters are mounted directly to the Spectrometer (Figure 8).

The Instrument Data Processing Unit, described by Curtis *et al.* (2002) (see Figures 9 and 10) contains all the remaining Spectrometer electronics. The signals from the CSAs are shaped, amplified, processed, and digitized by nine identical Detector Interface Boards (DIBs), one for each GeD. The DIBs feature (1) quasi-trapezoidal shaping to compensate for ballistic deficit effects of the charge collection in these large GeDs, (2) dual fast/slow signal processing chains for pulse-pileup rejection, and (3) ultrahigh rate counting in broad energy bands with the fast chain with live time measurements every 0.5 ms to preserve the imaging capability.

The GeD front segment energy range is ~ 3 keV up to ~ 2.7 MeV in 8192 channels with ~ 0.33 keV ch^{-1}. The rear segments cover from ~ 20 keV to ~ 2.7 MeV and have an additional low-gain slow amplifier to cover from ~ 2.7 MeV up to ~ 17 MeV (2.7 keV ch^{-1}). For each detected photon, 14 bits of energy information and the time of arrival to 1 microsecond are encoded together with detector identification and live time into a 24-bit event word. Normally every photon is stored in the spacecraft mass memory and then telemetered to the ground.
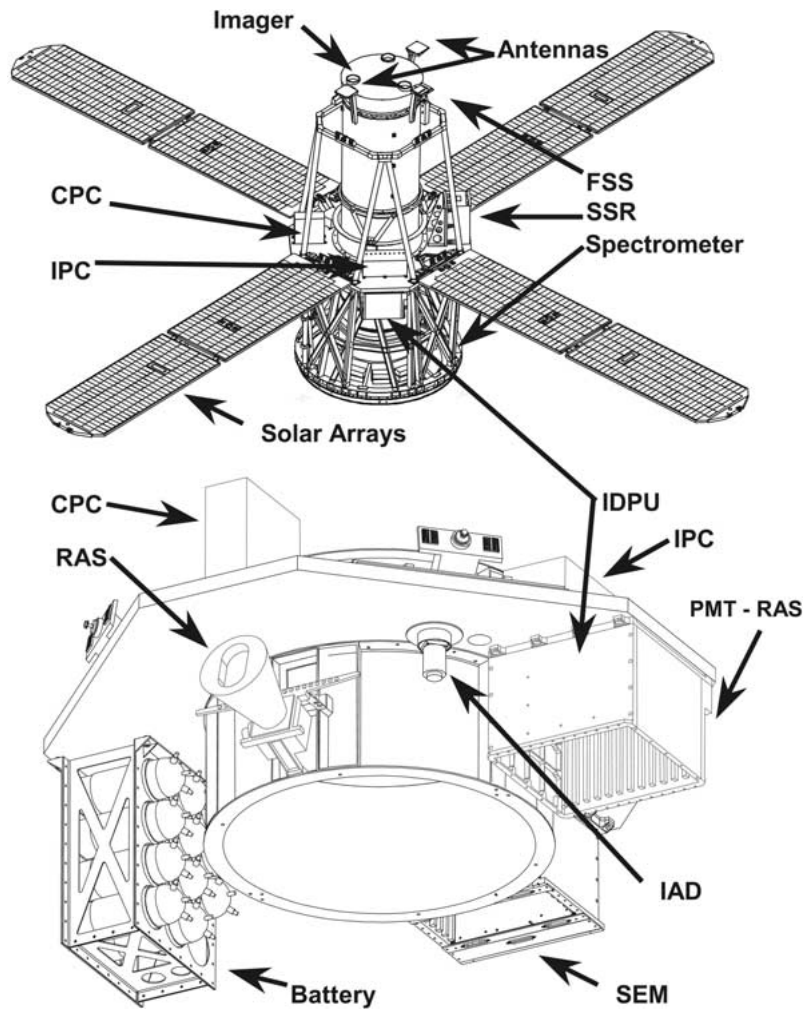
Figure 10. [See CD-ROM for color version]. Schematic showing the location of instrument and spacecraft components on the RHESSI spacecraft. The acronyms in the top view are: Fine Sun Sensor (FSS), Solid State Recorder (SSR), Cryocooler Power Converter (CPC), Instrument Power Converter (IPC), Instrument Data Processing Unit (IDPU); in the bottom view, Roll Angle System (RAS), Photomultiplier Roll Angle System (PMT RAS), Inertial Adjustment Device (IAD), Spacecraft Electronics Module (SEM).

A 300-micron thick, 1 cm^2 area, passivated-ion-implanted (PIP) silicon detector with a CSA/amp/discriminator electronics, similar to those flown on the Wind 3D Plasma and Energetic Particle instrument (Lin *et al.*, 1995), monitors energetic particle fluxes. The IDPU low voltage power converter provides the 100-V bias supply for the particle detector. Two discriminator levels provide measurements of energetic ($\gtrsim$ 1 MeV) electron and ($\gtrsim$ 10 MeV proton fluxes.

The Controller card collects and formats data from the DIBs and the particle detector, and passes the formatted data to the spacecraft over a high speed (>20 Mbps) bus. A microprocessor on the Controller card controls the IDPU, including the cooler and shutters, and interfaces to the spacecraft over a low speed serial interface for receipt of ground commands and exchange of housekeeping and status information.

A space-qualified power converter (CPC) consisting of two amplifiers was developed for the cryocooler. A pulse-width-modulated amplifier amplifies a temperature dependent IDPU-provided sine wave at 59.6 Hz to drive up to 100 watts peak into the voice-coil-like cryocooler load of $\sim 1.2\ \Omega$. The second amplifier, driven from an IDPU-provided phase-shifted temperature-dependent sine wave at the same frequency, powers the cryocooler counterbalancer to minimize microphonics.

An Instrument Power Controller (IPC) contains the low and high voltage converters for the instrument. The CPC and IPC are housed in physically separate boxes from the rest of the IDPU (Figure 10).

4. Spacecraft

4.1. STRUCTURE AND MECHANISMS

The RHESSI spacecraft bus (Figure 10) was designed and manufactured by Spectrum Astro, Inc. of Gilbert, AZ. The primary structure supports all spacecraft components during the launch environment and maintains the relative alignment of the Imager and the Spectrometer. Most of the spacecraft components are located on an octagonal aluminum honeycomb equipment deck that is mounted to the spacecraft aft ring. The Imager tube is supported around its center of gravity by three flexure mounts to a machined aluminum imager support ring mounted on the forward side of the equipment deck. The Spectrometer is attached to the spacecraft aft ring with its large thermal radiator flush with the launch vehicle separation plane for an unobstructed field of view.

The solar array consists of four identical wings, each with two panels connected by a hinge, located symmetrically around the equipment deck. A metal tip-mass at the end of each wing increases the deployed spin-axis moment of inertia for spinning stability. To align the spin axis closer to the imager boresight on orbit, the spacecraft spin balance can be fine-tuned with two controllable Inertia Adjustment Devices (IADs) – motorized linear drive screws that move two of the solar array wings. The mid-wing and root hinges of each solar array wing use steel tape-measure material to provide both the deployment force and a rigid latch in the deployed state. Shape Memory Alloy (SMA) actuated release devices preload the array panels against snubbers in the stowed configuration. These actuators stretch to snap the titanium tiedown bolts to release the wings. The solar cells are exposed

on the outboard panel so that some power is generated even before the panels are deployed.

4.2. ATTITUDE CONTROL

The Attitude Control Subsystem (ACS) enables RHESSI to follow the Sun over time autonomously with a 3σ pointing accuracy of 0.14° (8.4 arc min). The primary attitude sensor is an Adcole Inc. fine Sun sensor (FSS) with a $\pm 32°$ field of view and 0.005° resolution, that is mounted to the front of the imager tube. The pointing error measured by the FSS, together with local magnetic field measurements made by the spacecraft magnetometer, are inputs to the ACS control algorithms in the flight software. This runs on the RAD6000 flight processor in the Command and Data Handling (C&DH) subsystem to drive three orthogonally-mounted Ithaco Inc. 60 Ampère-meter^2 Electromagnetic Torque Rods to maintain the spacecraft attitude. Finally, a set of eight coarse sun sensor cells (two mounted on each solar array wing) allow the ACS subsystem to acquire the Sun from any initial attitude after separation from the launch vehicle.

The ACS flight software provides an Acquisition mode which damps rates after launch vehicle separation, a Precession mode which orients the spin axis toward the sun from any starting attitude, a Spin Control mode which adjusts the vehicle spin rate to a commandable value, and a Normal mode which is used during most mission operations to keep the spin axis pointed at the Sun. The ACS also has an Idle mode which does not actively control the vehicle attitude. Because RHESSI is designed to be a stable spinner, the idle mode provides a safe mode that is entered in the event of an anomaly. The ACS flight software is auto-coded using MatrixX software and integrated with the remainder of the flight software.

4.3. COMMAND AND DATA HANDLING

The Spacecraft Electronics Module (SEM, Figure 10) houses the Charge Control Board (CCB), the Power Control Board (PCB), and the Auxiliary Driver Board (ADB) for the Electrical Power Subsystem (EPS); and Communications Interface Board (CIB), the Payload and Attitude Control Interface (PACI) board, and the flight computer (CPU) board of the Command and Data Handling (C&DH) subsystem. A separate Solid State Recorder (SSR, Figure 10), built by SEAKR Engineering, provides 4 gigabytes of solid-state memory for science data storage.

The Instrument Data Processing Unit provides formatted telemetry packets of science data directly to the SSR recording high-speed parallel interface. Science data are played back from the SSR for downlink via a high-speed parallel interface with the CIB, the command and telemetry interface for the SEM to the RF transponder. The CIB is powered from the essential bus and is operational at all times. It provides command decoding capability for critical functions including the reset and power control of the flight computer, control of the telemetry transmitter, and adjustment of the battery charge control parameters. This hardware command

decoding capability of the CIB provides an operational backup for faults which result in the shutdown of CPU or software.

The Payload and Attitude Control Interface (PACI) board is responsible for telemetry encoding and data acquisition. It digitally encodes analog voltage, current and temperature data, and formats telemetry frames for downlink and on-board storage. It provides serial communications interfaces for control and monitoring of the SSR and the IDPU. The PACI board is powered by the essential power bus and is always producing hardware state of health telemetry packets; whenever the transmitter is powered on these packets are transmitted to the ground. This feature along with the CIB hardware command decoding, allows problems to be diagnosed and fixed from the ground, even without the CPU or software running.

The CPU board is a radiation-hardened RAD6000 processor made by BAE Systems. It contains 128 MB of DRAM for data memory storage and cache memory storage, and 3 MB of EEPROM for code memory storage. The CPU board controls the operation of all of the other boards in the SEM. The SEM also houses DC/DC power converters and an oven-controlled crystal oscillator (OCXO). The essential bus +28V power provided by the power subsystem is used to generate secondary +5V, and ±15V services which power the SEM boards. The OCXO provides a stable clock signal at a frequency of 2^{22} Hz, which is divided by the CIB to produce clock signals at 1 Hz and 2^{20} Hz (approximately 1 MHz). These signals are distributed to the CIB, the PACI, and the IDPU, where they are used to time-stamp data acquisition and frame transmission times.

4.4. FLIGHT SOFTWARE

The Flight Software is hosted on the CPU board. All software tasks execute under a VxWorks® Real Time Operating System, which handles software initialization and scheduling on a priority basis. Most tasks are scheduled to execute in one of three hardware generated cycle rates, the fastest of which is 8 Hz. ACS tasks are generally synchronous, while some C&DH tasks are triggered asynchronously by events. C&DH tasking performs all non-ACS spacecraft and payload functions including clock and schedule management, commanding validation and execution, telemetry collection/formatting, ground communication, power control, payload interfacing as required, and fault management.

4.5. ELECTRICAL POWER SUBSYSTEM (EPS)

The Electrical Power Subsystem (EPS) utilizes four triple-junction gallium arsenide (GaAs) solar array wings, each producing 133.5 W for a total of 534 W at 3 years end-of-life. Energy for eclipse operations is stored in a 15 Ampère-hour battery comprised of eleven common pressure vessels, each containing two nickel-hydrogen cells. The battery can operate at 50% depth-of-discharge for the full three year design life, and provide up to 280 W during the nominal 35-min eclipse duration. The Charge Control Board(CCB) uses a direct energy transfer system and

is better than 95% efficient. The amount of current produced by the solar array is controlled by pulse-width modulating FET switches between the eight solar cell circuits and the power bus. Unused solar array power is dissipated in the solar array, not in the spacecraft. The CCB uses a temperature-compensated battery voltage algorithm to set the battery charge current. The PCB distributes power to the spacecraft components and provides switched power to those components requiring unregulated power at $28+7/-4$ V. It also provides current sensors for telemetry monitoring and over-current protection for the power bus and under-voltage load shedding. The Auxiliary Driver Board (ADB) provides drive signals for the Inertia Adjustment Devices and the electromagnetic torque rods, and controls the solar array wing deployments

4.6. TELECOMMUNICATIONS

The Telecommunications subsystem provides S-band Radio Frequency (RF) links for telemetry and command. It includes an S-band transponder made by Cincinnati Electronics, an RF combiner, an RF switch, and four patch antennas located at the forward (Figure 10) and aft sections of the spacecraft which are combined and provide nearly 4π steradian uplink coverage. The system is capable of full duplex operation. Baseband data format is NRZM to eliminate phase ambiguities that can occur in the uplink and downlink receivers. Two kbps command data is BPSK modulated onto a 16 kHz sub-carrier on the main 2040 MHz carrier frequency. The downlink data rate is nominally 4.0 Mbps, and the frequency is 2215 MHz.

The receiver is 'hardwired' to the essential power bus and can never be switched off. The RF path to the receiver contains no switches in order to eliminate risk associated with failures. The transmitter is placed into standby mode or powered off between downlink activities through time tagged commands. The downlink signal is switched to either the forward or aft antenna to avoid interference. The ground provides time-tagged commands to select the best antenna based on the known sun-pointed vehicle attitude and the look-angle to the ground station. Link acquisition begins by transmission of a beacon with data transitions. Following downlink signal acquisition, the ground station transmits the uplink signal. The spacecraft is then commanded to transmit scientific data as well as normal state of health telemetry.

4.7. THERMAL CONTROL

The thermal control system for the spacecraft bus is a simple, cold-biased design using flight proven technologies. The thermal radiator surfaces are covered with 10 mil silver-coated teflon, and Multi-Layer Insulation blankets have a 2 mil, Indium Tin Oxide coated/reinforced second surface/kapton outboard layer, 0.25 mil aluminized Mylar inner layers with Dacron mesh separators. Active thermal components include kapton etched foil strip heaters controlled by bimetallic thermostats.
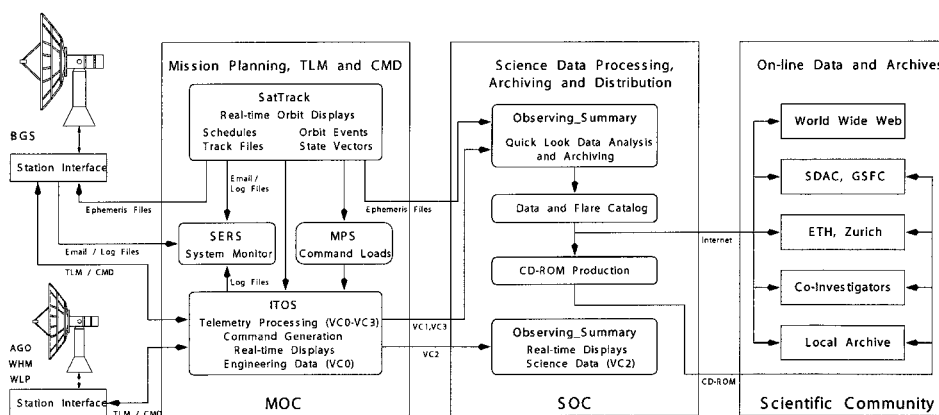
Figure 11. RHESSI ground data system.

The thermal performance in orbit matches the analytical predictions very well, with all components well within their design temperature ranges.

5. Mission Operations and Ground Data Systems

A schematic of the RHESSI Ground Data System (GDS) is shown in Figure 11. RHESSI is operated from the highly integrated and automated Mission Operations Center (MOC) located at Space Sciences Laboratory of the University of California at Berkeley. The MOC also supports the Fast Auroral Snapshot Explorer (FAST). Co-located with the multi-mission MOC are the RHESSI and FAST Science Operations Center (SOC) and the Berkeley Ground Station (BGS), the primary ground station to support RHESSI on-orbit.

5.1. MISSION OPERATIONS SYSTEMS

RHESSI is operated in store-and-dump mode. The spacecraft transmitter is turned on and off by time sequence commands stored on-board. These commands and many others related to configuring instruments for various phases of the orbit are part of an Absolute Time Sequence (ATS) load generated with the Mission Planning System (MPS). Command loads are uploaded to the spacecraft every two days and cover 4–5 days in advance.

The spacecraft command and control system for RHESSI is the Integrated Test and Operations System (ITOS). Since ITOS was also used during mission integration and testing, members of the Berkeley Flight Operations Team were trained early on operating the spacecraft. This approach allowed for a smooth transition from spacecraft integration and testing to normal on-orbit operations.

Flight dynamics and mission planning products are generated by the Berkeley Flight Dynamics System, which is based on the SatTrack Suite V4.4. SatTrack also

has heritage with various NASA missions and is used to generate all flight dynamics products such as ground station view periods, link access periods, terminator, high-latitude region, and South Atlantic Anomaly (SAA) crossings, and other orbit events needed as input to MPS. Other tools in the SatTrack Suite are employed to distribute real-time event messages to various ground data system elements such as ITOS and the BGS in an autonomous client/server network environment. SatTrack also provides a multitude of related automation functions as well as 2-D and 3-D real-time orbit displays.

All RHESSI space and ground systems are tied into the Spacecraft Emergency Response System (SERS), which is a data base system that regularly parses through log files and automatically checks for yellow or red limit violations. It also acts on warning and error messages received from various GDS subsystems via electronic mail. In case an anomaly is detected, the on-call operations team member is alerted via 2-way email pager in order to assess and resolve the situation. SERS completes the autonomous ground system and adds a high degree of reliability.

5.2. BERKELEY GROUND STATION (BGS)

The Berkeley Ground Station (BGS) is located adjacent to Space Sciences Laboratory. The antenna consists of a pedestal with an 11-m parabolic reflector. A three-axis drive system eliminates the keyhole at the zenith. The antenna is equipped with a full-duplex S-band telemetry and command system. The receiving system has a figure of merit (G/T) of 24.2 dB/K in each of the two receive channels (Left Hand and Right Hand Circular Polarization) for elevations above $5°$. The system uses dual receivers with diversity combination. A conical scan feed system provides autotrack capabilities with a typical accuracy of $0.1°$. The transmit polarization is selectable, and the nominal RF output power is 100 W (EIRP 63.0 dBW).

5.3. NORMAL OPERATIONS

During Normal Operations, communication with the spacecraft is established six times per day via the Berkeley Ground Station to monitor the spacecraft health and safety, and to retrieve science and engineering data. Scheduling and execution of these pass supports is performed fully autonomously. Routine orbit determination functions are carried out by USSPACECOM (formerly NORAD). Updated two-line element sets are automatically downloaded and archived twice a day in order to generate all tracking schedules and mission planning products.

The SatTrack Gateway Server at the Berkeley MOC invokes scripts that regenerate all mission planning products and contact schedules. The updated multi-mission pass support schedule is then loaded into the Gateway Server. Connected clients such as the BGS and various ITOS systems receive support request messages 10 minutes before a pass support. All systems then automatically configure themselves and open network connections for telemetry and command data flows. Once

the spacecraft rises above the horizon, the real-time pass support commences by establishing two-way communications with the spacecraft in order to perform health and safety checks and to download stored science and engineering data.

Upon completion of a pass support, the downloaded engineering data are examined for any system anomalies. Yellow or red limit violations trigger immediate notification of operations personnel via the Spacecraft Emergency Response System (SERS). Science data are automatically transferred from the ground station to the level-zero processing (LZP) system. Once LZP is completed, the data are transferred to their on-line archive at Berkeley. In addition, the automated CD-ROM production system will eventually produce multiple copies of the data.

5.4. BACK-UP TELEMETRY AND COMMAND SUPPORT

Three additional ground stations are used regularly to provide additional telemetry and/or command support. These ground stations are the Wallops Island ground station in Virginia, operated by NASA, the Weilheim ground station in Germany, operated by DLR, and the Santiago ground station in Chile, operated by the University of Santiago. A dedicated T-1 line from the Berkeley Mission Operations Center to Goddard Space Flight Center, which is shared with the FAST project, is used to establish secure real-time communications with the RHESSI spacecraft through the Wallops ground station. Telemetry data received and stored at the ground stations are transferred to Berkeley post-pass via the open Internet. The averaged link access for the Berkeley and Wallops 11-m ground stations is 55 min day^{-1}. Santiago can provide an additional 51 min day^{-1}, and Weilheim 16 min day^{-1}.

The RHESSI ground system was designed to recover all the data (except for periods of major flare activity) with 6 Berkeley passes daily, but the solar fluxes in the previously unexplored 3–20 keV range, the terrestrial precipitation at L = 2–2.5, and the background were all higher than anticipated. Thus, typically 4 additional passes, taken at any of the other three stations, are required to recover all the data.

6. Science Operations and Data Analysis

6.1. SCIENCE OPERATIONS

RHESSI operations have been designed from the start to be largely autonomous with minimum input in terms of different operating mode or observing plans. All systems are designed to operate automatically with no manual intervention. The main operations task is the management of the on-board solid-state recorder (SSR) during periods of high solar activity or when sufficient ground station dumps are not available to keep the SSR from filling up. When strong flare activity appears likely, we try to keep the SSR below ∼ 20% full at the end of the Berkeley passes, so that there is plenty of capacity remaining for a big X-class flare. An attenuator

can be inserted by command to reduce the incoming soft X-ray flux, or some of the data in the SSR can be skipped and not telemetered down.

A team scientist, modeled on the *Yohkoh* 'Tohban' role, monitors solar activity and the instrument operation daily to ensure that the observations are being taken to maximize the scientific return. The Tohban also coordinates with other observatories and notes any special campaign-style observations that may be ongoing to ensure the optimum interchange of information.

The data are generally available for analysis from one to three days after the observation is made. Once the instrument data are recorded in the SSR, it takes up to two days to be telemetered to a ground station depending on how full the SSR becomes. Once on the ground at Berkeley, the packetized data files are converted to Flexible Image Transport System (FITS) format and stored on a Redundant Array of Independent Disks (RAID) system. They are then transmitted over the Internet to Goddard, where they are stored on a similar RAID system. The data are also stored at the HESSI Experimental Data Center (HEDC) at ETH Zurich. At this point, all the data are freely available for downloading by outside users without restriction.

6.2. DATA ANALYSIS

RHESSI differs from many imagers in that, instead of transmitting a preselected subset of images, the telemetry includes all of the information about each detected photon. Thus, the data analyst can make tradeoffs among time resolution, spectral range and resolution, spatial resolution, image quality, etc., on the ground. These decisions can be made on a case-by-case basis to match the unique characteristics of the event under study and the relevant scientific objective. A key driver of the RHESSI data analysis approach is the preservation of this flexibility to extract the maximum scientific return from the observations. This means that all detailed scientific analysis will use the same primary database with the most current calibration information.

Furthermore, (1) the complete data output of the RHESSI mission is made available promptly to the scientific community, without restriction; and (2) a fully documented analysis package, supported by a range of platforms, is available to the scientific community, with the same toolbox of software used by the PI team. A promptly-generated catalog of summary data products is distributed with the RHESSI data base, to serve as a multi-parameter index and overview of the data base, and to provide data products to users not requiring custom analyses.

The data analysis software is described in the accompanying paper by Schwartz *et al.* (2002). It is also freely available and can be conveniently downloaded as part of the Solar Software (SSW) tree. The extensive RHESSI software package, mostly written in the Interactive Data Language (IDL) programming language, contains all procedures necessary to read the FITS data files, prepare and plot light curves, images, and spectra, and output the results for further customized analysis.

Furthermore, the joint analysis of many different observations of the same events by other observatories is greatly facilitated, since most other solar space missions and many ground-based observatories also have their analysis software in this same SSW tree. A convenient interface is provided to allow easy comparison of RHESSI images and light curves with similar products from SOHO, TRACE, GOES, Big Bear Observatory, etc. The analysis procedures can all be invoked from the IDL command line, or a more user-friendly graphical user interface is also available for basic analysis tasks. All the software is fully compatible with both the Unix and Windows operating systems. The SSW system allows for rapid bug fixes and software upgrades that can be downloaded to each user's own computer at any time from a central server, several of which exist in different countries around the world. For users without IDL, the HEDC provides internet browser software to access and analyze the data.

In an effort to familiarize as many interested scientists as possible with analyzing RHESSI observations, three data analysis workshops have been held. These provided training to about thirty scientists at each workshop in accessing RHESSI data and in the use of the image reconstruction and spectral analysis software. On-line documentation is available for all the software from beginner guides to the detailed manuals required by program developers. This documentation can be accessed through the following web site:

http://hesperia.gsfc.nasa.gov/rhessidatacenter/.

7. Summary

On 12 February 2002, one week after launch, the germanium detectors were turned on after being cooled down to their operating temperature range by the cryocooler, and RHESSI detected its first flare, a C2 GOES event at 02:14 UT. Since then, RHESSI has been operating continously, and through the end of August 2002, it had detected over 1900 flares above 12 keV and over 600 above 25 keV. It has provided the first imaging spectroscopy of solar flares. It has detected the first 3–10 keV hard X-ray microflares, and found that the Sun is continually emitting hard X-rays above ~ 3 keV. On 23 July it obtained the first high-resolution spectrum of solar gamma-ray lines and the first images of a gamma-ray line, from a GOES X4.8 flare.

As indicated by the early results papers in this issue, RHESSI is already providing many exciting new results, particularly gratifying given the many travails the project suffered pre-launch. However, the power of RHESSI lies in its capability for detailed quantitative probing of the particle acceleration and energy release mechanism. That will require careful, comprehensive analysis of the RHESSI data, together with the context measurements from other spacecraft and from the ground.

Acknowledgements

References

Bougeret, J.-L. *et al.*: 1995, *Space Sci. Rev.* **71**, 231.
Chupp, E. L.: 1990, *Phys. Scripta* **T18**, 15.
Curtis, D. W. *et al.*: 2002, *Solar Phys.*, this volume.
Emslie, G., Brown, J. C. and MacKinnon, A. L.: 1997, *Astrophys. J.* **485**.
Fishman, G. *et al.*: 1994, *Science* **264**, 1313.
Harmon, B. A. *et al.*: 1992, *Proc. of the CGRO Workshop*, p. 69.
Hurford, G. J. and D. W. Curtis: 2002, *Solar Phys.*, this volume.
Hurford, G. J. *et al.*: 2002, *Solar Phys.*, this volume.
Johns, C. and Lin, R. P.: 1992, *Solar Phys.* **137**, 121.
Kosugi, T. *et al.*: 1991, *Solar Phys.* **136**, 17.
Lin, R. P. and Hudson, H. S.: 1976, *Solar Phys.* **50**, 153.
Lin, R. P. *et al.*: 1995, *Space Sci. Rev.* **71**, 125.
Makashima, K. *et al.*: 1977, in K. A. van der Hucht and G. Vaiana (eds.), *New Instrumentation for Space Astronomy*, Pergamon Press, New York.
Prince, T. A. *et al.*: 1998, *Solar Phys.* **118**, 269.
Ramaty, R. and Murphy, R. J.: 1987, *Space Sci. Rev.* **45**, 213.
Ramaty, R. *et al.*: 1993, *Adv. Space Res.* **13**, 275.
Ramaty, R., Mandzhavidze, N., Kozlovsky, B. and Murphy, R. J.: 1995, *Astrophys. J.* **455**, L193.
Schwartz, R. *et al.*: 2002, *Solar Phys.*, this volume.
Share, G. H. and Murphy, R. J.: 1995, *Astrophys. J.* **452**, 933.
Smith, D. M. *et al.*: 2002, *Solar Phys.*, this volume.
Zehnder, A. *et al.*: 2002, *Solar Phys.*, this volume.
Zhang, S. N., Fishman, G. J., Harmon, B. A. and Paciesas, W. S.: 1993, *Nature* **366**, 245.